THE MECHANISM OF GAS TRANSPORT IN HUMAN RESPIRATORY CYCLE AND ITS APPLICATION TO EFFICIENT MASS AND HEAT TRANSPORT DEVICES

Sadanari MOCHIZUKI
Department of Mechanical Systems Engineering, Tokyo University of A&T,
Koganei, Tokyo 184-8588, Japan, *Tel./Fax. +81(0)42-388-7088,* motizuki@cc.tuat.ac.jp

Abstract *The first half of the present paper deals with the experimental study on the gas exchange mechanism during the respiratory cycle in human lungs. In order to simulate the airway structure of the human lungs, a regular dichotomy bronchial tube model (of Weibel) of four generations was employed. The flow of the working fluid, water, was visualized using dye as the tracer illuminated by fluorescent light. The results showed that the reciprocating flow and branching tube network is a marvelous combination which enables bi-directional mass transport in conducting airways of human lungs, and that the bi-directional mass transport is attributed to the "trap and release" mechanism based on the "formation and destruction" of separated flow region. Based on this newly found phenomenon of "trap and release", the second half of the present paper deals with the study on heat transport in reciprocating flow inside ribbed circular tubes. This study was conducted with an attempt to explore an efficient heat transport tube where the heat is transported from one end to the other of the tube with extremely high heat transport performance.*

Key words: *human lung, branching tubes, reciprocating flow, bi-directional mass transport, heat transport*

1. INTRODUCTION

The airway of the human lung consists of a very complicated branching tube network, as shown in Fig. 1. The trachea branches and forms bronchi. At each bronchus, the airways repeat branching with their average diameter and the length decreasing. A typical model representing the structure of the human lung is a symmetrical dichotomy model by Weibel [1] as shown in Fig.2. At the end of airways, there are numerous alveoli which exchange carbon dioxide for oxygen. The airways from the trachea to 14th-15th generations are called the conducting airways which do not participate in the direct gas exchange with the blood.

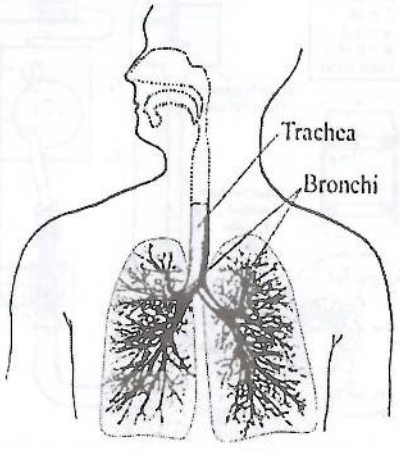

Fig. 1 Conceptual Illustration of Human Lung

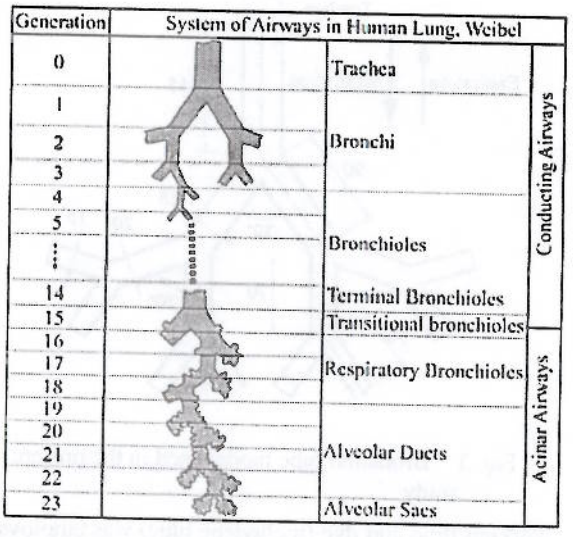

Fig. 2 Schematic of Weibel's dichotomy model for airways in human lung

As for the gas transport in the conducting airways, a lot of researches have been done. Extensive reviews [2],[3] and books [4],[5] were published. However, the mechanism how the fresh air, which was inhaled in the inspiration process, reaches alveoli is not understood well yet.

In normal respiration, although the volume of air inspired into the lung is about 1/3 of the entire capacity of the lung, the fresh air reaches alveoli and exchange oxygen for carbon dioxide. Gas transport is known to be sustained when the ventilation frequency is kept high even if the volume of air inspired into the lung is only about 1/30 of the entire capacity of the lung. This is called HFV (High Frequency Ventilation). Since one end of the airway system (trachea) is open to the atmosphere and the other ends of the system (alveoli) are blind alleys, for fresh air and old air to reach the alveoli and the trachea, respectively, they must be exchanged or swapped in every passage.

2. EXPERIMENTAL APPARATUS

2.1 Flow visualization for a branching tube network and a ribbed straight tube

Figure 3 illustrates the test section used in the present study. It was a regular dichotomy model of four generations with the branching angle of 70 degrees. It was fabricated with glass tubes and corresponds to L_i/d_i=3.5, d_{i+1}/d_i=0.78 and ϕ =70 deg, where L_i, d_i and ϕ denote length, diameter and branching angel of tubes of the i-th generation, respectively.

The experimental apparatus is shown in Fig. 4. It consists of a branching-tube-network model, a water tank with transparent acrylic fiber wall, a settling chamber, a dye reservoir, a reciprocating-flow generator, a light source and a digital video camera. Water was used as the

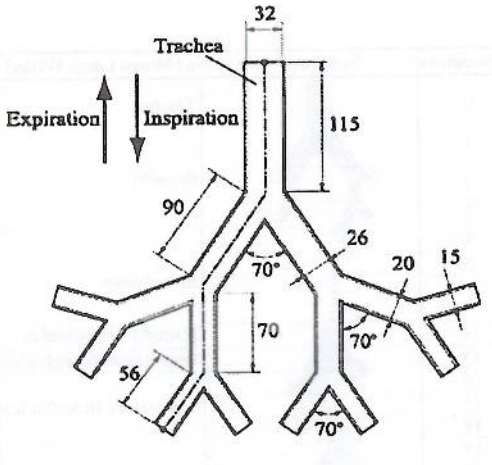

Fig. 3 Bronchial tube model used in the present study

working fluid and dye (methylene blue) was employed as the tracer to visualize the behavior of the flow.

The whole test section is submerged and the test section exits are open to the water in the tank. Before each run of the experiment, dye was stored in the dye reservoir using an injector, and the reciprocating-flow generator was set in motion. The frequency f of the reciprocating flow was changed by setting the turning speed of the motor. The stroke volume (often called tidal volume in the research field of the lung) V_T was varied by choosing the number of the syringes.

Visualized flow was recorded by the digital-video camera under the illumination from the fluorescence light source which was installed under the water tank. The

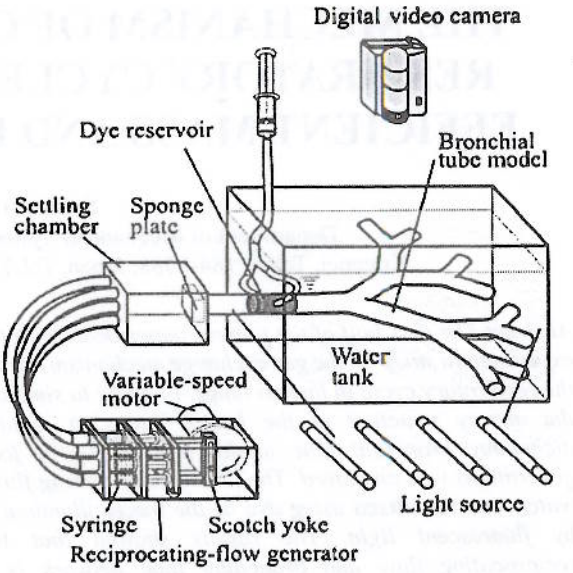

Fig. 4 Schematic of experimental setup for flow visualization in branching tubes

experiment was conducted in the range where the Reynolds number was Re_0 =60-6000 and dimensionless frequency or Womersley Number was $Wo = (d/2)(2\pi f/\nu)^{1/2}$ =5-25. In the case of usual human ventilation, Re_0 and Wo are approximately 1000 and 3, respectively. For High Frequency Ventilation, they are about 2000 and 20, respectively.

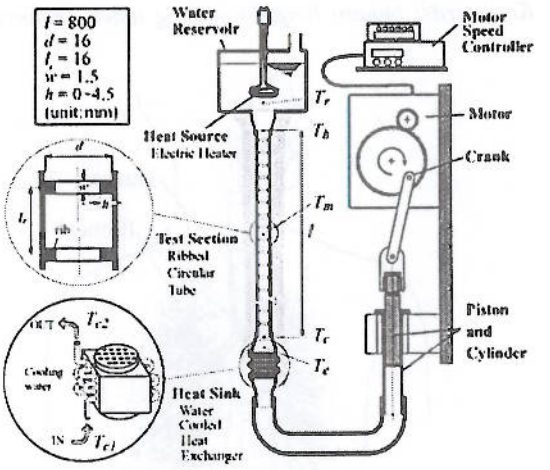

Fig. 5 Schematic of Experimental Setup for Heat Transport inside a ribbed Tube

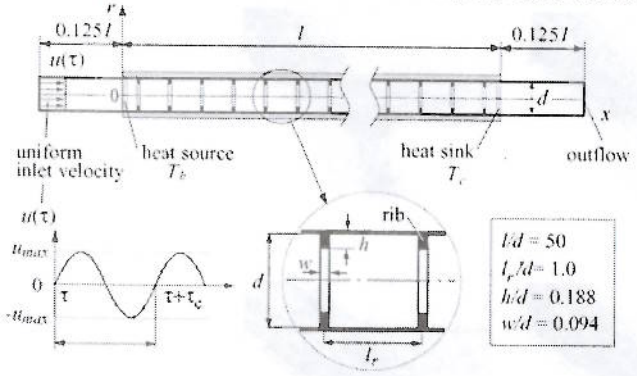

Fig. 6 Numerical Simulation Model of a Heat Transport Tube

2.2 Experimental setup for heat transport in ribbed tubes

The experimental set-up for heat transport in a single straight tube is shown in Fig. 5. It consists of a vertically arranged test section (ribbed circular tube), hot water reservoir with heater, heat sink, piston-crank mechanism, variable speed motor and its controller. Water is used as working fluid. The inner diameter and the length of the test section are d = 16 mm and l = 800 mm, respectively. Annular ribs whose cross section is rectangular (width w = 1.5 mm, height h =1.5, 3.0 and 4.5 mm, varied) are installed with the axial pitch l_r = 16 mm. Temperatures at various points were measured by thermocouples and the volume flow rate of the cooling water was measured by a mess cylinder and a stop watch. Sinusoidal change in flow rate was realized by the piston-crank mechanism. Experiments were conducted in the range of stroke l_s 14.6 220 [mm] and frequency f =0.15Hz 1.0Hz. The heat transport rate from the heat source to the heat sink was obtained from

$$\dot{Q} = \rho_w c_p \dot{V} (T_{c2} - T_{c1}) \qquad (1)$$

where ρ_w c_p $\dot{V}$ T_{c1} and T_{c2} are density, specific heat, volume flow rate, outlet temperature and inlet temperature of the cooling water at the heat sink heat exchanger.

In the present study, effective thermal conductivity was introduced as a measure of heat transport performance of the tube. It is defined by the following equation.

$$k_{eff} = \frac{\dot{Q}l}{(T_h - T_c)} \cdot \frac{4}{\pi d^2} \qquad (2)$$

3. NUMERICAL SIMULATION OF FLUID FLOW AND HEAT TRANSPORT IN RIBBED TUBES

Numerical simulation was conducted using commercially available software (FLUENT 6.2). Under the assumption of axisymmetrical, two dimensional, incompressible and unsteady flow, equations of continuity, momentum and energy were solved numerically. As is shown in Fig. 6, starting sections for flow with length 0.125l was provided at the both ends of the test section. At the inlet of the test section (x/l = -0.125), uniform velocity distribution over the cross section which changes sinusoidally with time was given as

$$u(\tau) = u_{max} \sin(2\pi f \tau) \quad \pi f l_s \sin(2\pi f \tau) \qquad (3)$$

Heat source and sink were set at x/l=0 and x/l=1, and the fluid which passed those location was set to T_h and T_c, respectively. Adiabatic condition was imposed on the entire wall surface including rib surfaces. As the Reynolds number based on the mean velocity ($2fl_s$) and tube diameter d is in the range of 2500 to 15000 in the present study, standard k-ε model is employed.

4. RESULTS AND DISCUSSION

4.1 Branching Tube Network

Some examples of the visualized results recorded from the top of the test section are shown in Fig. 7(a)-(f) for $Re_0 = u_m d/\nu$=800 and $Wo = (d/2)(2\pi f/\nu)^{1/2}$=12. These photographs indicate flow situation at the beginning of inspiration or expiration processes of each cycle over the period of 2.5 cycles. The timings of photography for (a) to (f) in Fig.7 correspond, respectively, to the marks (a) to (f) in the top of Fig.7. In each photo, the dark part designates the portion of fluid colored by the dye. Comparing to the human ventilation, the colored fluid will be called "fresh air" and transparent fluid will be called "old air". The fresh air which was initially at the entrance (see Fig.7 (a)) of the 0-th generation tube (the trachea) reaches the entrance region of the second generation tube at the end of the

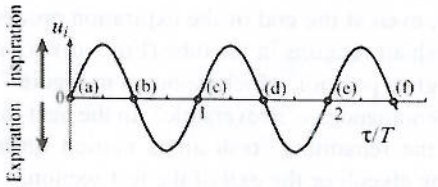

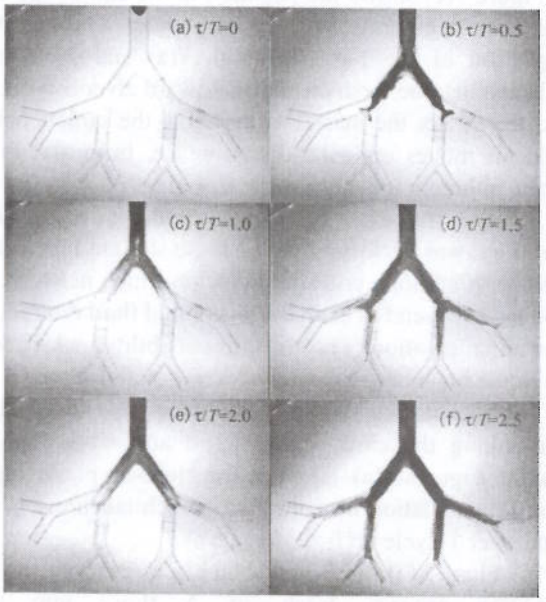

Fig. 7 Axial propagation of mass originally at the entrance of the trachea tube, Re_0=800, α_0=12

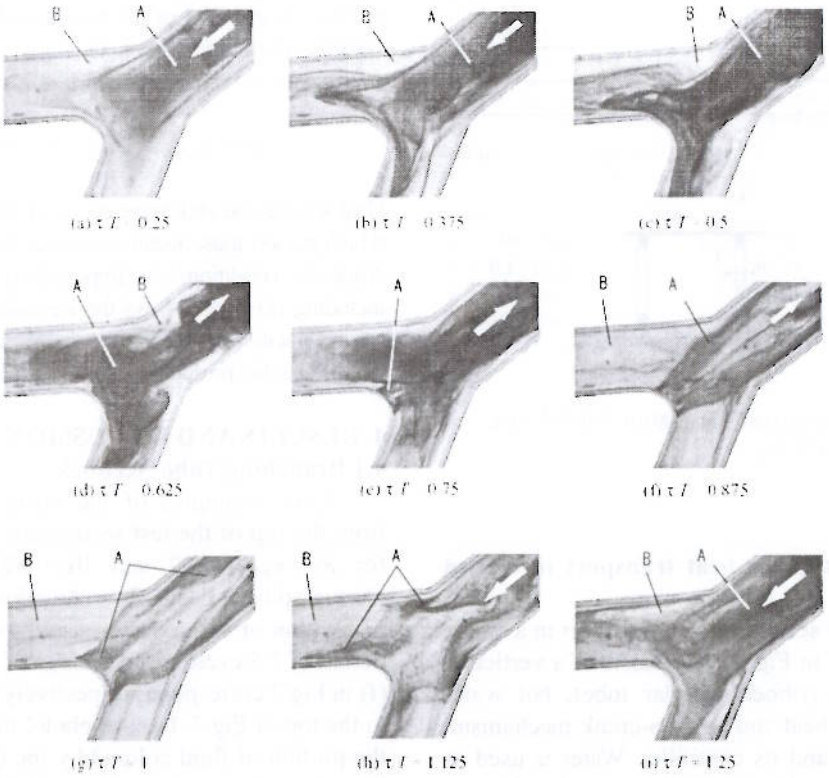

Fig. 8 Visualized flow behavior at the 2nd branch during the period of one cycle

inspiration process (Fig.7 (b)). In the following expiration process, the fresh air moves back toward the trachea. However, even at the end of the expiration process, a part of the fresh air remains in the tube (Fig.7(c)) not returning to the original position which is shown in Figure 7(a). That is, the phenomenon is "irreversible". In the next inspiration process, the remaining fresh air is carried further down toward the alveoli or the exit of the test section.

Figure 7(e) shows the situation at the end of the 2nd cycle, i.e. beginning of the 3rd cycle. Through the comparison of the Fig. 7(e) with 7(a) and 7(c), it is confirmed that the fresh air moves toward alveoli cycle by cycle. To satisfy the mass conservation, the same amount of old air moves opposite direction, i.e. from alveoli to trachea, although it is not visible from Fig. 7.

In the present research, similar visualization experiment was performed for a single straight tube under the same conditions with the branching tube network. In this case, at the end of each cycle, colored fluid returned to the original position. That is, "irreversibility" which was seen in the branching tube network was not observed.

The mechanism of the phenomenon is examined in detail taking the case of Re_0=1190 and Wo=12 as an example. Figures 8(a)~(i) show the close-up photographs of the flow situation near the 2nd branch taken every 1/8 period over 1-cycle (t/T=0.25~1.25).

In Figs. 8(a) and (b) which correspond to the inspiration process, fresh air A flows into two 2nd-generation tubes which branch from the 1st-generation tube. The flow separation occurs in the bent wall, that is, on the walls of the outside of those 2nd-generation tubes. Old air B is being trapped within these separation regions. When the inspiration process ends (Fig. 8(c)), the mean flow velocity becomes zero. However, because of the inertial force, the fluid in the central core region still keeps moving towards the alveoli, while the fluid near the wall flows towards the trachea resulting in the extinction of the separation phenomenon and old air B which has been trapped in the separation region starts to move towards the trachea. In the expiration process, when the entire fluid heads for the trachea, the old air B is rapidly entrained by the flow towards the trachea (Figs. 8 (d) and (e)).

The separation occurs also in the expiration process. In this case, the fresh air A is trapped in the separation region (Figs. 8 (e), (f) and (g)). The separation in the expiration process occurs at two different places, one is at the intersection of the two different-diameter tubes (i.e., daughter and parent tubes) and the other is at the downstream of the bent wall as was observed in the inspiration process. They are coexisting and connected with each other. When the expiration process ends (Fig. 8 (g)) and the inspiration process starts again, the fresh air A which has been trapped in the separation region begins to move quickly towards the alveoli (Fig. 8 (h)). Figure 8 (i) shows the flow at the end of one complete cycle which started at t/T=0.25 (Fig. 8 (a)).

From the description above, one can conclude that the mechanism of the axially bidirectional mass transport in the reciprocating flow in the branching tube network is attributed to "trap-and-release" which is based on the "generation-and-extinction" of the flow separation regions.

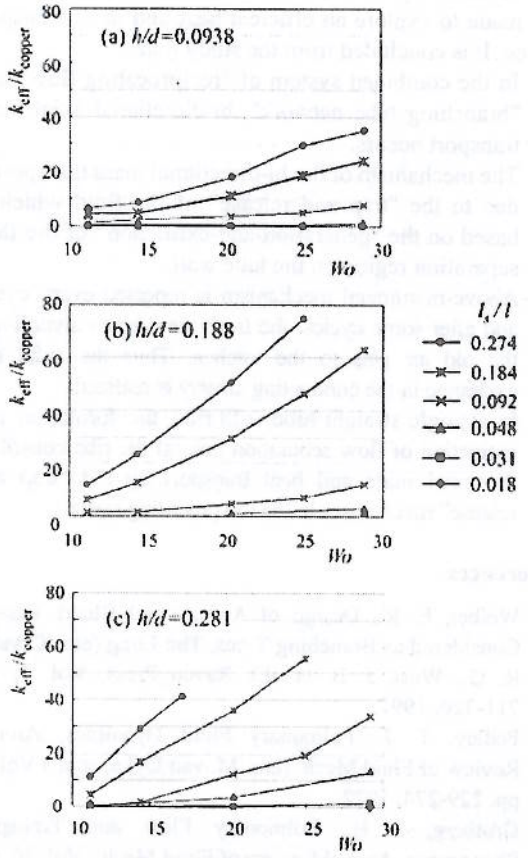

Fig. 9 Experimental Results of Heat Transport for Ribbed Tubes

That is, in the inspiration process, old air is trapped in the separation regions. However, in the consecutive expiration process, with the extinction of the separation phenomenon, it is released and entrained by the flow heading towards trachea. On the other hand, in the expiration process, fresh air is trapped within the separation regions. This fresh air is released in the following inspiration process and carried by the flow towards the alveoli. Such a mechanism is repeated in every cycle. As a result, after some cycles, the fresh air reaches alveoli and the old air gets to the trachea.

4.2 Ribbed Circular Tubes

It was suggested by the above study that the combination of reciprocating flow and the flow separation may bring about bi-directional axial mass and heat transport. With an attempt to realize an efficient heat transport device based on this result, experimental and numerical studies were performed to clarify the axial mass and heat transport mechanism of reciprocating flow inside ribbed circular tubes, where the ribs were attached as flow separation inducers.

Figures 9 (a)-(c) show experimental results of heat transport performance, k_{eff}/k_{copper}, for three different rib height (h/d =0.0938 □0.188 and 0.2.81) plotted against Womersley number, $Wo=(d/2)(2\pi f/\nu)^{1/2}$ with dimensionless stroke (l_s/l) as a parameter. From the figures, one can understand that :

(1) Irrespective to h/d and l_s/l, k_{eff}/k_{copper} increases monotonically with an increase in Wo□

(2) Irrespective to h/d and Wo, k_{eff}/k_{copper} increases monotonically with an increase in l_s/l□

A comparison of experimental and numerical results for the cases of l_s/l =0.184 and 0.274 are shown in Fig. 10. One can see that the results of numerical simulation agree very well with those of experiment, verifying the numerical simulation conducted in the present study gives reliable results.

In Figs.11(a)-(e), time-dependent velocity vectors for smooth tube and ribbed tube at x/l=0.49□0.51 are compared over a half cycle for the case of a Wo=29.1 (f=1Hz) and l_s/l=0.184 (l_s=147mm). As is well known, in the case of smooth tube, there exists phase lag in the velocity behavior between the core region and near-wall region. This is the main cause of the axial heat transport for the case of smooth tube (or so-called "dream pipe").

On the other hand, in the case of ribbed tube, flow behavior is much more complex because of the formation of flow separation region in between the ribs as one can observe in the figures at right column of Fig.11. In the case (a) of Fig. (11), cross-sectional mean velocity is zero. When the fluid starts to move toward right direction (b), the fluid in the core region flows into the near-wall region in between the ribs sweeping the fluid which has been trapped in that region. As the mean velocity increases (c), the near-wall region between the adjacent ribs is occupied by the separation bubbles in which the trapped fluid is recirculating. The mean fluid velocity decreases gradually (d), and eventually it becomes zero (e). The similar situation is repeated with the direction of velocity inverted in the latter half of the cycle. As is shown above, fluid is trapped and released corresponding to the formation and extinction of the flow separation region.

Fig. 12 shows some examples of mass (tracer) dispersion characteristics obtained through numerical simulation. Tracer is fed at the entrance (x=0) periodically with a small time interval and its dispersion characteristics are shown at three time phases for smooth tube (first three figures of Fig. 13) and ribbed tube (latter three figures). It is clearly shown that in the case of ribbed tube, the tracer disperses from left to right every cycle while in the case of smooth tube, the tracer does not disperse just making a reciprocating motion with almost the same stroke with that of a virtual piston. From the law of mass conservation, it is obvious that to compensate the mass (tracer) flow from left to right, the same amount of mass is flowing from right to left. It can be

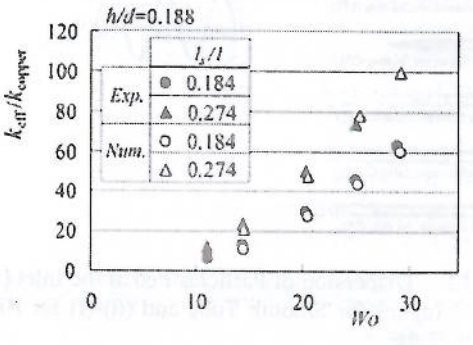

Fig.10 Comparison of Experimental and Numerical Simulation Results

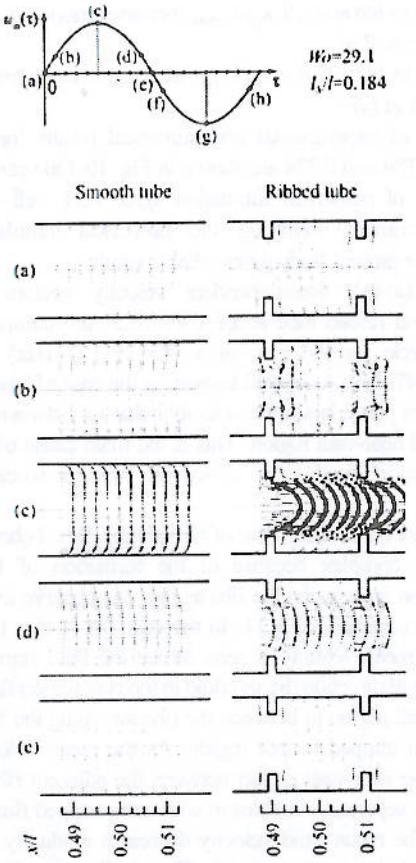

Fig. 11 Change of Velocity Vectors with Time for Smooth and Ribbed Tubes.

concluded that the reciprocating flow inside a ribbed tube creates bi-directional mass transport which is caused by the "trap and release" mechanism based on the "formation and extinction" of separation region.

5. CONCLUSIONS

Flow visualization experiment was performed for the reciprocating fluid flow in the branching tube network to clarify the gas exchange mechanism in the conducting airways of human lung. Based on the mechanism which was revealed by the above mentioned study, an attempt was made to explore an efficient heat and mass transport device. It is concluded from the study that:

(1) In the combined system of "reciprocating flow" and "branching tube network", bi-directional axial mass transport occurs.

(2) The mechanism of the bi-directional mass transport is due to the "trap and release" of the fluid which is based on the "generation-and-extinction" of the flow separation region on the tube wall.

(3) Above-mentioned mechanism is repeated every cycle, and after some cycles, the fresh air reaches alveoli and the old air gets to the trachea. Thus the axial gas exchange in the conducting airway is realized.

(4) In a single straight tube with ribs, the formation and extinction of flow separation behind the ribs constitute the axial mass and heat transport by the "trap and release" mechanism in the reciprocating cycle.

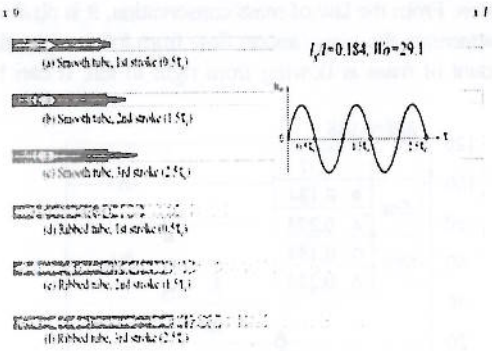

Fig. 12 Dispersion of Particles Fed at the Inlet (x=0), (a)-(c) for Smooth Tube and (d)-(f) for Ribbed Tube

References

[1] Weibel, E. R., Design of Airway and Blood Vessels Considered as Branching Trees, The Lung (eds. Crystal, R. G., West, J. B. et al.), Raven Press, Vol. 1, pp. 711-720, 1991.

[2] Pedley, T. J., Pulmonary Fluid Dynamics, Annual Review of Fluid Mech. (eds. M. van Dyke, et al.) Vol. 9, pp. 229-274, 1977.

[3] Grotberg, J. B., Pulmonary Flow and Transport Phenomena, Annual Review of Fluid Mech., Vol. 26, pp. 529-571, 1994.

[4] Ultman, J. S., Gas Mixing and Distribution in the Lung (eds. Engel, L. A. and Paiva, M.), Marcell Dekker, Inc., NY, pp. 63-136, 1985

[5] Crystal, R. G., The Lung, Raven Press Inc. ,1991

[6] Kurzweg, U. H. and Zhao, L.-d., Heat Transfer by High-Frequency Oscillations: A New Hydrodynamic Technique for Achieving Large Effective Thermal Conductivities, Physics Fluids, Vol. 27, No. 11 (1984), pp. 2624-2627.

[7] Kaviany, M., Performance of a Heat Exchanger Based on Enhanced Heat Diffusion in Fluids by Oscillation: Analysis, Transaction of the ASME, Journal of Heat Transfer, Vol.112 (1990), pp.49-55.

[8] Kaviany, M. and Reckker, M., Performance of a Heat Exchanger Based on Enhanced Heat Diffusion in Fluids by Oscillation: Experiment, Transaction of the ASME, Journal of Heat Transfer, Vol.112 (1990), pp.56-63.

[9] Nishio, S. et al., Oscillation-Controlled Heat Transport Tube (1st Report, Effect of Liquid Properties), Transaction of the Japan Society of Mechanical Engineers, Series B, Vol. 60, No. 569 (1994), pp. 233-239.